Spectral narrowing and stabilization of thulium fiber lasers using guided-mode resonance filters

R. Andrew Sims,[1,*] Zachary A. Roth,[2] Christina C. C. Willis,[1] Pankaj Kadwani,[1] Timothy S. McComb,[1] Lawrence Shah,[1] Vikas Sudesh,[1,3] Menelaos Poutous,[2] Eric G. Johnson,[2] and Martin Richardson[1]

[1]*Townes Laser Institute, CREOL College of Optics and Photonics, University of Central Florida, 4000 Central Florida Boulevard, Orlando, Florida 32816, USA*

[2]*The Center for Optoelectronics and Optical Communications, University of North Carolina at Charlotte, 9201 University City Boulevard, Charlotte, North Carolina 28223, USA*

[3]*Currently with Quantum Technology, Inc., 108 Commerce Street, Suite 102, Lake Mary, Florida 32746, USA*

**Corresponding author: rasims@creol.ucf.edu*

Received October 26, 2010; revised December 9, 2010; accepted January 10, 2011; posted February 7, 2011 (Doc. ID 137253); published February 28, 2011

We used guided-mode resonance filters (GMRFs), fabricated using thin-film deposition and chemical etching, as intracavity feedback elements to stabilize and narrow the output spectrum in thulium-doped fiber oscillators operating in the 2 μm wavelength regime, producing linewidths of <700 pm up to 10 W power levels. A Tm fiber-based amplified spontaneous emission source was used to characterize the reflective properties of the GMRFs. Linewidths of 500 pm and a 7.3 dB reduction in transmission were measured on resonances.

OCIS codes: 140.3510, 140.3425.

Thulium's wide emission spectrum (1.8–2.1 μm) and ease of diode pumping, due to a cross-relaxation process [1], make it an excellent fiber dopant ion. Good thermal and power handling properties allow thulium fiber lasers to operate at high powers with a nearly diffraction-limited beam quality. Many important applications for Tm fiber lasers, such as tissue ablation [2] and lidar [3] overlap the laser emission with narrow absorption resonances, which requires precise wavelength control and narrow linewidths. Narrow and stabilized spectral output is also important for spectral beam combining (SBC), an important technique for scaling power beyond what is possible from a single fiber laser aperture without sacrificing beam quality [4,5]. Due to the immaturity of 2 μm components relative to 1 and 1.5 μm, there is a strong need for new or improved components, particularly to stabilize the wavelength and narrow linewidth.

Fiber Bragg gratings (FBGs) are the most common components used for wavelength stabilization in fiber lasers [6]. FBGs can be easily spliced into fiber laser systems and engineered to provide reflectivities from ~10% to >99%. FBGs are compatible with high average powers, and heating or mechanically stressing the FBG can tune the output wavelength. While this approach is technologically mature for single-mode fiber applications [6], FBGs for large mode area fibers have a relatively broad spectral output associated with multiple transverse modes lasing as determined by the fiber parameters [7]. However, significantly narrower linewidths are required for the aforementioned applications.

Established free-space wavelength control methods include diffraction gratings and volume Bragg gratings (VBGs). A plane ruled reflection grating can be incorporated easily into an oscillator cavity to provide both wavelength tuning and stabilization, but it has several drawbacks, including relatively low diffraction efficiency, the requirement for relatively long free-space cavity sections to minimize the output linewidth, and an inability to maintain subnanometer spectra at higher powers due to thermally induced distortions, particularly with conventional metal-coated gratings [8]. VBGs are free-space optical elements recorded in photothermorefractive (PTR) glass as volumetric holographic gratings. VBGs offer high reflectivity, wide wavelength tunability, and narrow linewidth [9], and they have been used to stabilize fiber laser oscillators at 1, 1.5, and 2 μm wavelengths at output powers of >100 W with no efficiency degradation [10–12]; however, laser-induced heating in the PTR glass during high-power operation can cause wavelength shifts of ~0.1 nm for an estimated 15° temperature increase [10].

Here we demonstrate guided-mode resonance filters (GMRFs) as feedback elements in thulium fiber oscillators. GMRFs have been demonstrated to watt-level average powers in Er-Yb fiber lasers operating at 1540 nm [13] and employed as feedback elements for seed lasers in Tm-doped amplifier systems used in preliminary SBC work at 2 μm wavelengths [14]. GMRFs can achieve high reflectivities (>99%), narrow spectral linewidths (<0.1 nm), and they can be fabricated at a relatively low cost in high quantities [13].

A GMRF is a metaoptical component that resonantly couples evanescent light into "leaky" waveguide modes, capable of producing highly efficient reflection peaks with a narrow linewidth [15]. GMRF devices, used in this study, are composed of two dielectric thin-film layers fabricated by thin-film deposition on a passive substrate. The top layer consists of a subwavelength grating (SWG) etched into the thin film, which diffracts light into the evanescent mode for wavelengths larger than the grating spatial period. The layer below the SWG is a waveguide or confinement layer. The highly efficient reflection is the result of coupling between the diffracted evanescent modes of the SWG and the leaky modes of the waveguide layer [16]. Performance of these components depends on several structural parameters: grating period and duty

0146-9592/11/050737-03$15.00/0

cycle; grating layer thickness; waveguide layer thickness; and the refractive indices of the grating, waveguide, and substrate materials. These design parameters provide many ways to engineer the GMRF performance.

The GMRFs used in this Letter had a 1 mm thick fused silica substrate coated using plasma enhanced chemical vapor deposition with 395 nm of silicon nitride (Si_xN_y) and 380 nm of silicon oxide (SiO_x). The former thin film is used as the confinement layer, and the latter as the grating layer. A hexagonal SWG was etched (130 nm depth) into the oxide film using standard microlithography. Fabrication errors, due to process control and deviation, have been shown to shift the resonance peak location to shorter wavelengths without affecting the linewidth significantly [17]. The hexagonal symmetry of the grating layer produces a polarization insensitive GMRF with the reflection spectra of both polarizations overlapping [18].

We characterized the performance of the GMRF using a setup based upon a 4 m long section of Tm-doped (~4 wt.%) fiber with a 25 μm diameter, 0.09 NA core and a 400 μm diameter, 0.46 NA octagonal cladding (Nufern). The active fiber was coiled around an aluminum water-cooled heat-sink at ~14 °C in order to maintain high cross-relaxation efficiency. The Tm fiber was spliced to a passive fiber of matching dimensions for thermal management during end pumping. To manage heat in the fiber facets and polymer coating, the ends of the passive fiber were secured in water-cooled copper V grooves.

The Tm fiber was pumped with a 790 nm fiber-coupled laser diode. Pump light was coupled through a pair of 100 mm focal length achromatic lenses and reflected from an angled dichroic mirror (HR 0.8 μm, HT 2 μm) into a flat-cleaved fiber facet. The ~4% Fresnel reflection from the flat-cleaved fiber facet serves as the output coupler for the resonator. The opposite fiber facet was angle cleaved at ~8° in order to suppress parasitic lasing, and the output was collimated with a 26 mm AR coated Infrasil aplanatic triplet lens to the GMRF.

Using the schematic shown in Fig. 1, the pump power was set just below the laser threshold, such that the system served as a broadband amplified spontaneous emission (ASE) source. The ASE spectrum was recorded with an optical spectrum analyzer [(OSA) Yokagawa AQ6370] prior to inserting the GMRF in the beam path. With the GMRF placed into the beam path as shown, pump power was increased to above the lasing threshold and the GMRF was aligned to provide cavity feedback with maximum laser efficiency and spectral stability. Pump power was then reduced to below the threshold level, and the ASE spectrum transmitted through the GMRF was recorded.

The data show that when the GMRF is optimized for feedback in the laser cavity, the orthogonal polarizations of ASE encounter two different resonances. The reflectivity is centered at 2013.12 nm with a spectral width of 1.89 nm FWHM. The maximum reflectivity of the two peaks is ~2.25 dB or ~40% (assuming all loss is due to reflection). While viewing the ASE transmission, it is possible to align the GMRF such that both polarizations share a single reflection peak that is narrower and of higher contrast. As shown in Fig. 2, in this case the center wavelength is 2013.12 nm with a spectral width of ~500 pm (FWHM) and the minimum of transmission is −7.3 dB (~81%). However, this configuration does not provide feedback for laser oscillation, indicating that the incident light is not normal to the GMRF. When aligned for cavity feedback, polarization splitting occurred due to the off-normal, or nonplanar, incidence causing asymmetric mode coupling into the confinement layer and thus splitting the effective resonances.

Using the GMRF as the feedback element for spectral narrowing and wavelength stabilization, output powers up to 10 W were realized, above which parasitic lasing generated multiple wavelengths outside the resonance envelope of the GMRF. The GMRF based cavity had a ~34% slope efficiency with respect to launched pump power as measured from a single output. Including the leakage through the GMRF yields ~40% slope efficiency, which suggests that improved GMRF reflectivity will increase laser efficiency.

The spectral output was dependent on the output power of the laser (Fig. 3). Initial laser oscillations occurred at 2013.70 nm with a spectral FWHM of 0.18 nm. As power was increased, a wavelength shift occurred up to 2014.02 nm and increased to a width of 0.40 nm. At 10 W output power, two laser peaks were observed due to the orthogonal polarizations, causing feedback and resulting in a net linewidth of 0.70 nm. Laser wavelength shifts remain within the reflective envelope determined by the GMRF (Fig. 2). This wavelength shift and

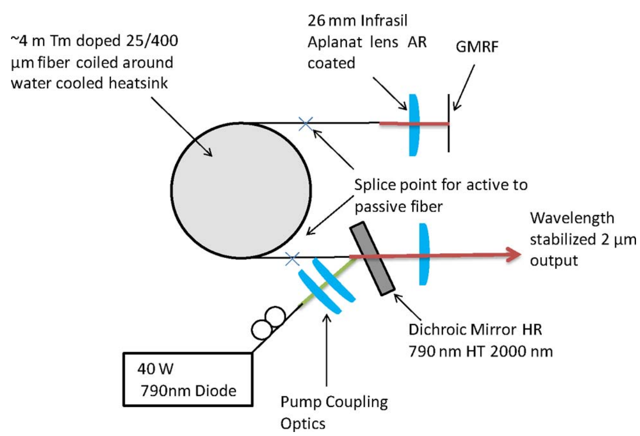

Fig. 1. (Color online) Schematic of the Tm laser setup that was used for GMRF characterization and laser operation.

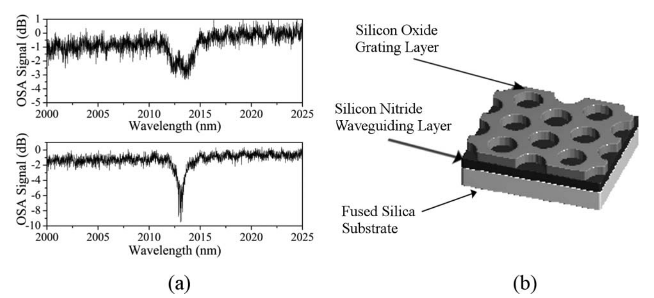

Fig. 2. (a) Transmission graphs of ASE through the GMRF. The top shows the GMRF operating on two polarizations, while the bottom shows by alignment the polarization collapses to a single peak with higher reflectivity. (b) Computer drawing of the structure of the GMRF.

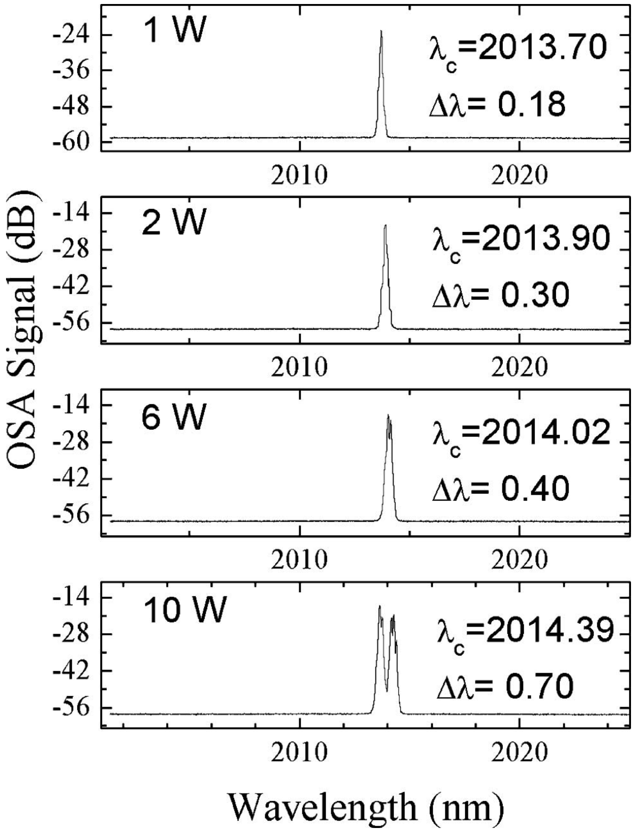

Fig. 3. Spectral evolution of the laser at four different power levels. At the 10 W power level, the spectrum begins to expand due to the presence of two polarizations.

spectral broadening is due to the inhomogeneously broadened nature of Tm and gain competition within the spectral reflection. If parasitic lasing were better suppressed, we expect that the spectrum would continue broadening with increasing power until the reflective envelope is filled.

Presently, the most prominent limitation inhibiting power scaling to multiple 100 W is the low reflectivity. GMRFs with reflectivities of >99% have been fabricated [13], and work toward a higher reflectivity polarization-insensitive GMRF is ongoing. Also, polarization-sensitive designs could be used in conjunction with PM fiber to achieve a polarized output.

We have demonstrated a 10 W wavelength stabilized oscillator—the highest output power yet achieved using a GMRF for intracavity feedback. Power levels and laser efficiencies were limited due to the low reflectivity around 2 μm, but GMRF technology at other wavelength regimes has proven that higher reflectivity is possible. Spectral shifts due to laser dynamics within the GMRF reflectivity envelope are seen as a function of power from levels of 1 to 10 W, but would be significantly reduced with a narrower resonant linewidth. Work is currently under way to improve GMRF fabrication, particularly to optimize the design parameters to increase reflectivity, reduce the resonant linewidth, and improve angular selectivity with the goal to stabilize Tm fiber lasers to multi-100 W power levels with sub-100 pm linewidths.

This work was supported by the High Energy Laser Joint Technology Office through the MRI program (contract W911NF-05-1-0517), and the authors wish to acknowledge the support of Nufern, Inc., and the states of Florida and North Carolina.

References

1. S. D. Jackson, Opt. Commun. **230**, 197 (2004).
2. N. M. Fried, Lasers Surg. Med. **37**, 53 (2005).
3. G. J. Koch, J. Y. Beyon, B. W. Barnes, M. Petro, J. Yu, F. Amzajerdian, M. J. Kavaya, and U. N. Singh, Opt. Eng. **46**, 116201 (2007).
4. S. J. Augst, A. K. Goyal, R. L. Aggarwal, T. Y. Fan, and A. Sanchez, Opt. Lett. **28**, 331 (2003).
5. J. W. Dawson, M. J. Messerly, R. J. Beach, M. Y. Shverdin, E. A. Stappaerts, A. K. Sridharan, P. H. Pax, J. E. Heebner, C. W. Siders, and C. P. J. Barty, Opt. Express **16**, 13240 (2008).
6. T. Erdogan, J. Lightwave Technol. **15**, 1277 (1997).
7. C.-H. Liu, A. Galvanauskas, V. Khitrov, B. Samson, U. Manyam, K. Tankala, D. Machewirth, and S. Heinemann, Opt. Lett. **31**, 17 (2006).
8. D. Y. Shen, J. K. Sahu, and W. A. Clarkson, Opt. Express **13**, 4916 (2005).
9. O. M. Efimov, L. B. Glebov, L. N. Glebova, K. C. Richardson, and V. I. Smirnov, Appl. Opt. **38**, 619 (1999).
10. P. Jelger, P. Wang, J. K. Sahu, F. Laurell, and W. A. Clarkson, Opt. Express **16**, 9507 (2008).
11. J. W. Kim, P. Jelger, J. K. Sahu, F. Laurell, and W. A. Clarkson, Opt. Lett. **33**, 1204 (2008).
12. F. Wang, D. Shen, D. Fan, and Q. Lu, Opt. Express **18**, 8937.
13. A. A. Mehta, R. C. Rumpf, Z. A. Roth, and E. G. Johnson, IEEE Photon. Technol. Lett. **19**, 2030 (2007).
14. R. A. Sims, C. C. C. Willis, P. Kadwani, T. S. McComb, V. Sudesh, R. Zachary, M. Poutous, E. G. Johnson, and M. Richardson, Opt. Commun. 284 1988 (2010).
15. R. Magnusson and S. S. Wang, Appl. Phys. Lett. **61**, 1022 (1992).
16. A.-L. Fehrembach, D. Maystre, and A. Sentenac, J. Opt. Soc. Am. A **19**, 1136 (2002).
17. M. K. Poutous, Z. Roth, K. Buhl, A. Pung, R. C. Rumpf, and E. G. Johnson, Proc. SPIE **7205**, 72050Y (2009).
18. A.-L. Fehrembach and A. Sentenac, J. Opt. Soc. Am. A **20**, 481 (2003).